journal

J. Am. Ceram. Soc., 93 [9] 2679–2683 (2010)
DOI: 10.1111/j.1551-2916.2010.03817.x

Nanostructured Forsterite Coating Strengthens Porous Hydroxyapatite for Bone Tissue Engineering

Rahmatollah Emadi,† Fariborz Tavangarian, Saied Iman Roohani Esfahani, Adel Sheikhhosseini, and Mahshid Kharaziha

Department of Materials Engineering, Isfahan University of Technology, Isfahan 84156-83111, Iran

Many attempts have been focused on preparing highly porous scaffolds with appropriate mechanical strength. This paper has developed a new route to enhance the compressive strength of porous hydroxyapatite (HA) scaffold (porosity: ~83%, mean pore size: ~740 μm). Briefly, this route included a nanostructure coating of forsterite (Mg_2SiO_4) on struts of porous HA. The coating microstructure consisted of the grains with the range between 35 and 80 nm and nanosize pores that could be detected by scanning electron microscopy observation. This simple method improved the compressive strength of highly porous HA from 0.12 to 1.61 MPa. The scaffolds obtained provided a good mechanical support while maintaining bioactivity, and hence they could be used as tissue engineering scaffolds for low-load-bearing applications.

I. Introduction

Tissue engineering offers a promising new approach to regenerate diseased or injured tissues such as bone.[1] For this issue, three-dimensional biocompatible porous scaffolds with a highly interconnected porosity are designed. Porous scaffold ceramics were developed to prevent the loosening of implants. The growth of bone into the surface porosity provides a large interfacial area between the implant and its host. This method of attachment is often called biological fixation. It is capable of withstanding more complex stress states than other kinds of implants. Furthermore, porous scaffold implants allow cell migration, vascularization, and diffusion of nutrients. On the other hand, they form a mechanical bond via ingrowth of bone into the pores.[2–5] From a macroscopic point of view, bone tissue is nonhomogeneous, porous, and anisotropic. Two types of bone tissue can be distinguished: trabecular or cancellous and cortical or compact. It is feasible to design the porosity of the materials to be similar to that of trabecular bone, which has a 50%–95% of porosity and a network of interconnected pores.[3]

In this sense, it is of great interest to obtain pore diameters of a hundred microns[6–8] and a number of designed pore interconnections to verify in the shortest possible time a bioresorption of the scaffold and the subsequent new bone formation. For this purpose, it is necessary to design highly porous scaffolds, which must include the necessary macroporosity to ensure bone oxygenation and angiogenesis.[8] Therefore, designed porous scaffolds should have a network of interconnected pores where more than 60% of pores should have a size ranging from 150 to 400 μm and, at least 20% should be smaller than 20 μm. Pores with sizes <1 μm are appropriate to interact with proteins and are mainly responsible for bioactivity. On the other hand, pores with sizes between 1 and 20 μm are important in cellular development, type of cells attracted, and the orientation and directionality of cellular ingrowth. Moreover, pores of sizes between 100 and 1000 μm play an important role in cellular and bone ingrowth, being necessary for blood flow distribution and having a predominant function in the mechanical strength of the substrate. Finally, the presence of pores of sizes >1000 μm will have an important role in the implant functionality and in its shape and esthetics. Consequently, porosity of three-dimensional scaffolds is a very important matter due to its great influence on the implant final behavior.[8] Although, hydroxyapatite (HA) is one of the most biocompatible materials with respect to human hard tissues, the low fracture toughness of HA ceramic limits the scope of clinical usages in load-bearing applications.[9,10] The porous forms of HA have also been widely used as bone scaffolds that provide improved bone ingrowth and osteointegration.[5,11,12] Damien *et al.*[13] evaluated the bioactivity of a novel synthetic porous hydroxyapatite (PHA) *in vivo* in rabbit and investigated the enhancement of its bioactivity and osteointegration. However, when a HA scaffold is fabricated by different routes, its porosity is limited to about 70%, because of the low mechanical properties of HA. In order to promote bone ingrowth and the vascularization of the newly formed tissue, scaffolds with a higher porosity are needed.[14]

Scaffolds should have suitable architecture and strength to serve their intended function. Highly porous ceramic scaffolds have been synthesized by various techniques including conventional, mainly manual techniques and advanced processing methods such as the rapid prototyping techniques as reviewed by Yeong *et al.*[15] Gross and Rodríguez-Lorenzo[16] developed a new technique for producing controlled pore shape and pore size interconnectivity. Salt particles were spheroidized in a flame and sintered to provide an interconnecting salt template. The salt template was filled with a carbonated fluorapatite powder and a polylactic polymer to produce a composite scaffold.[16]

Several attempts have been made to use strong materials, such as zirconia and alumina, as a supporting framework on which the HA layer is coated, which would provide a high strength as well as excellent biocompatibility.[17,18] Various efforts have been also carried out for the improvement of mechanical properties of highly porous ceramic scaffolds.[19–27] In recent years, some Si- and Mg-containing ceramics have drawn interests in the development of bone implant materials.[28–31]

Ni *et al.*[32] showed good biocompatibility and improved mechanical property of forsterite in comparison with HA. Kharaziha and Fathi[33] showed that forsterite nanopowder is bioactive. Also, they showed that nanocrystalline forsterite has higher mechanical properties than HA.[34] The aim of this work was to develop a new route to enhance the compression strength of highly PHA scaffold by nanostructured forsterite coating on HA struts.

II. Materials and Methods

(1) Preparation of HA Scaffolds

The spongy bone was extracted from a bovine bone and then cut into rectangular samples of an approximate size of 10 mm × 5 mm × 5 mm. The bone samples were annealed in an electric

H.-E. Kim—contributing editor

Manuscript No. 26852. Received September 21, 2009; approved March 29, 2010.
†Author to whom correspondence should be addressed. e-mail: remadi@cc.iut.ac.ir

furnace, under ambient condition, at 1000°C temperature for 2 h with a heating/cooling rate of 1°C/min.

(2) Preparation of Forsterite Powder

The flowchart shown in Fig. 1 outlines the experimental procedure used to synthesize the forsterite nanopowder described in our previous report.[34] In brief, water-based solutions of the magnesium salts and colloidal silica were prepared. An aqueous solution of sucrose was added to the solution. PVA solution was added to the final solution and the pH value was adjusted to 1. The solution was mixed homogeneously and heated at 80°C for 2 h. The prepared gel was then heated at 100°C in air for complete dehydration. In order to obtain pure forsterite nanopowder, the dried gel was calcined in a furnace at 700°–1000°C for 2 h.

The crystallite size of the forsterite powder was determined using the Scherrer equation

$$\beta = \frac{K\lambda}{t\cos\theta} \quad (1)$$

where λ is the wavelength (= 0.15406 nm), θ is the Bragg angle, k is a constant (= 0.9), and t is the apparent crystallite size. For this purpose, three diffraction peaks (211), (222), and (400), which have the advantage of being well separated and have high intensities, were chosen for the measurement. The half-widths were calculated using sigma plot software.

(3) Scaffold Coating

The slurry for the impregnation of the HA scaffolds was prepared by using the following recipe: PVA was dissolved in distilled water (0.01 mol/L). Then, forsterite powder was added to the solution, up to a concentration of 15 wt%. Each procedure was carried out under mild stirring using a magnetic stirrer for 2 h. The HA scaffolds with nearly the same porosity and pore size were immersed in the prepared slurry and remained in it for 1 h. The coated scaffolds were then placed on a ceramic plate and dried at ambient temperature for at least 12 h. After drying, scaffolds were sintered at 900°, 1000°, and 1100°C temperatures with 2 h of holding time. The heating and cooling rates were 2° and 5°C/min, respectively. The flowchart shown in Fig. 2 outlines the experimental procedure used for coating the scaffolds.

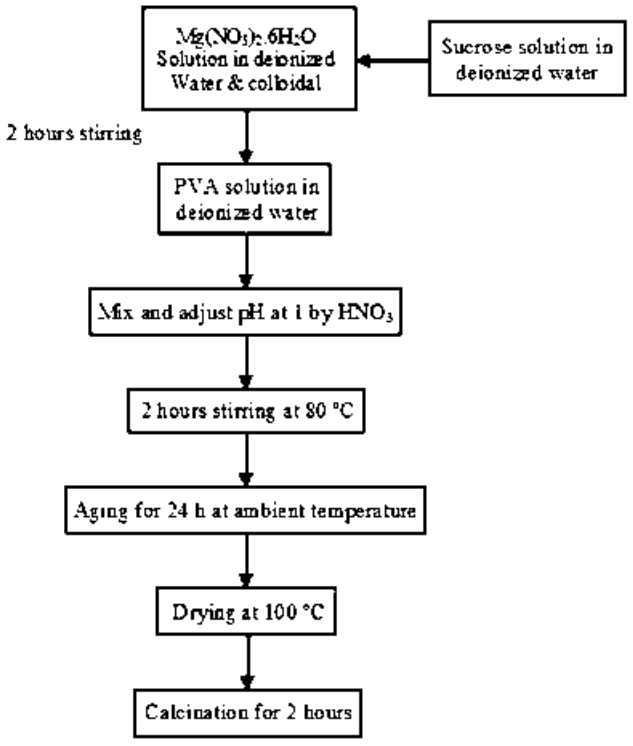

Fig. 1. Schematic flow chart of the synthesis of forsterite nanopowder.

(4) Scaffold Characterization

The scaffolds obtained were characterized by X-ray diffraction (XRD) and scanning electron microscopy coupled with energy-dispersive spectrometer. Image analysis method was used for the measurement of coating grains and mean size of pores. The porosity of scaffolds was measured according to the Archimedes principle.[35] The compressive strength of the scaffolds was measured using a universal testing machine (AG-400NL, Shimadzu Co., Nakagyo-ku, Kyoto, Japan) at a crosshead speed of 0.5 mm/min. Table I shows the structural characteristics and the mechanical properties of the scaffolds that prepared in this study.

III. Results and Discussion

Figure 3 illustrates XRD patterns of as-received and calcined precursor at different temperatures. The precursor is essentially amorphous. It can be observed that forsterite forms at 700°C while it is poorly crystallized. Periclase (MgO) peaks can be detected in samples calcined at 700°C, but only forsterite peaks can be seen in the powder calcined at higher temperatures (800°–1000°C).

Table II shows the crystallite size of forsterite calcined between 800° and 1000°C as to determined by the XRD line-broadening technique. As the calcination temperature increases, the size of the crystallite increases, as shown in Table II. The results showed that nanocrystallite forsterite powder had an average crystallite size in the range of 17–20 nm for the powders that calcined at 800°C for 2 h.

Figure 4 presents the XRD patterns of porous ceramics and prepared forsterite powder that sintered at different temperatures. The XRD pattern of the prepared powder displayed the formation of forsterite obtained by calcining at 800°C temperature (PDF #34-0189). All the XRD patterns obtained for the scaffolds were in agreement with the stoichiometric HA characterized pattern (XRD JCPDS data file No. 09-432). The XRD patterns of coated scaffolds (SC-800, SC-900, and SC-1000) were almost similar and exhibited an increase in peak height and a decrease in peak width as the sintering temperature increased, thus indicating an increase in crystallinity and crystallite size. XRD analysis could not identify the coating material because of the low amount of the forsterite. In addition, a peak

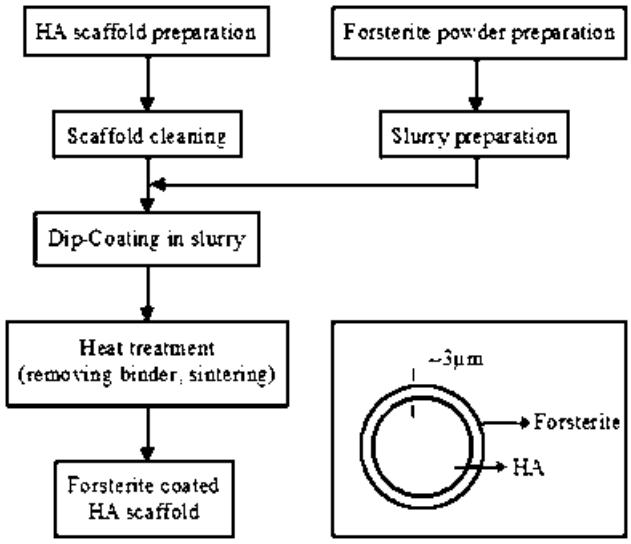

Fig. 2. Flow chart of the method used for the fabrication of hydroxyapatite (HA) scaffolds coated with forsterite. The inset illustrates the schematic of the cross section of the HA strut coated with forsterite.

Table I. Designations, Structural Characteristics, and Mechanical Properties of Porous Ceramics

Designation	Fabrication route	Porosity (%)	Mean pore size (μm)	Mean window size (μm)	Compressive strength (MPa)	Coating grain size minimum–maximum (nm)
SC-HA	Sintering bovine bone at 1000°C for 2 h	83.1±0.2	745	323	0.12±0.1	—
SC-1100	Forsterite coating on SC-HA and sintering at 1100°C for 2 h	82.2±0.2	750	320	1.61±0.03	1100–2300
SC-1000	Forsterite coating on SC-HA and sintering at 1000°C for 2 h	84.9±0.2	780	230	1.23±0.04	230–360
SC-900	Forsterite coating on SC-HA and sintering at 900°C for 2 h	80.8±0.2	710	210	0.57±0.04	35–80

corresponding to β-tricalcium phosphate (β-TCP) also appeared, indicating that some of the HA phase used as the framework was transformed into the TCP phase, due to its chemical reaction with the forsterite during sintering. It is shown that magnesium can stabilize the β-TCP phase at higher temperatures and promote the decomposition of HA.[36,37]

According to the Table I, as the sintering temperature increased to 1100°C, the compressive strength of scaffolds enhanced from 0.12 to 1.61 MPa. Figure 5 shows the pore structure and microstructure of the SC-1100. As shown in Fig. 5(a), the fabricated scaffold showed a reticulated structure, in which the pores were completely interconnected. The thickness of the coating layer was approximately 3 μm (Fig. 5(b)). The typical cross section of the scaffold is shown in Fig. 5(b); a uniform forsterite coating layer was formed on the HA struts with good interfacial bonding, presumably due to the chemical reaction. No cracks or interfacial delamination were observed. Elemental analysis of the coating layer exhibited the presence of silicon and magnesium, as shown in Fig. 5(b). The pore structure and microstructure of the HA scaffolds, before and after the coating are shown in Figs. 6(a)–(f). All scaffolds exhibited a pore size of ~750 μm and a porosity of ~83%. Figure 6(d) exhibits the microstructure of the SC-900 scaffold after the coating, which consisted of ultra-fine grain and many nanopores. Fine crystalline grains ranging between 35 and 80 nm could be detected. The dramatic change in the average grain size with the increasing of the sintering temperature is shown in Fig. 6(f). It was found that initially the grain size of the coating increased from ~60 nm at 900°C to about 300 nm at 1000°C and thereafter increased to ~2 μm when sintered at 1100°C. This observation confirmed the finding of Ramesh *et al.*[38] that some dramatic grain growth could be observed during the sintering of ultra-fine structures. It was found that SC-1100 samples with an average grain size of 2 μm and a mean micropore size of 500 nm exhibited the highest compressive strength.

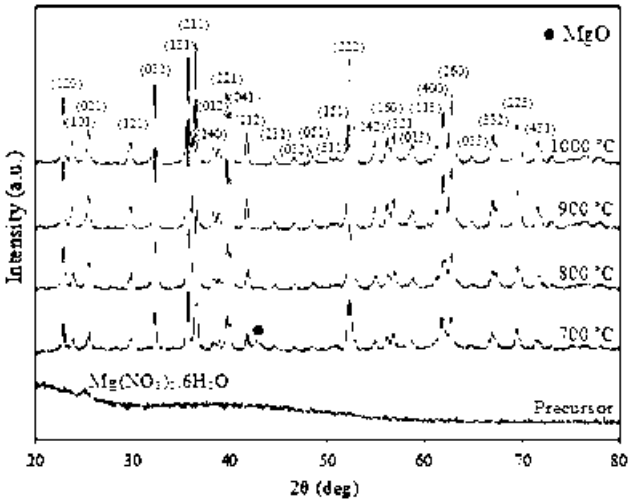

Fig. 3. X-ray diffraction patterns of as-received and calcined precursor at different temperatures (all of peaks are forsterite).

Table II. The Approximate Crystallite Size and Characteristics of the Forsterite Powder Calcined at Different Temperatures

System	T (°C)	d_{211}(Å)	D (nm)	d_{222} (Å)	D (nm)	d_{400} (Å)	D (nm)
A	800	2.457	20	1.748	17	1.495	18
A	900	2.457	23	1.748	19	1.495	21
A	1000	2.457	27	1.748	19	1.495	23

Scaffolds prepared using this method are very similar to spongy bone as compared with reports on the mechanical property and pore structure of cancellous bone.[19,20] The compressive strength of spongy bone is in the range of 0.2–4 MPa. The measured compressive strength (0.57–1.61 MPa) of the present coated foams falls in this range, and hence the present forsterite-coated HA scaffolds possess such an appropriate mechanical competence. There are some reports available on strength enhancement of highly porous HA (80%–90%).[23–27] Tian *et al.*[25] improved the compressive strength of porous HA (~82.46%) from 0.34 to 0.8 MPa by developing PLLA onto the framework of sintered HA scaffold. Kim *et al.*[26] developed a highly porous HA (~86%) by the polymer-sponge method with a compressive strength of 0.21 MPa. In another work, these researchers[27] developed a composite coatings (PA/poly(ε-caprolactone)) on the PHA and enhanced the compressive strength to 0.45. Jun *et al.*[24] fabricated PHA scaffolds coated with bioactive

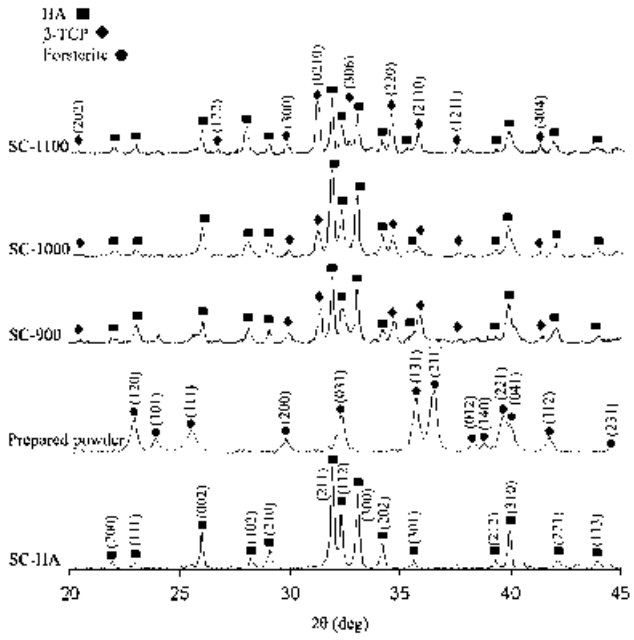

Fig. 4. X-ray diffraction patterns of SC-HA, SC-1100, SC-1000, SC-900, and prepared forsterite powder.

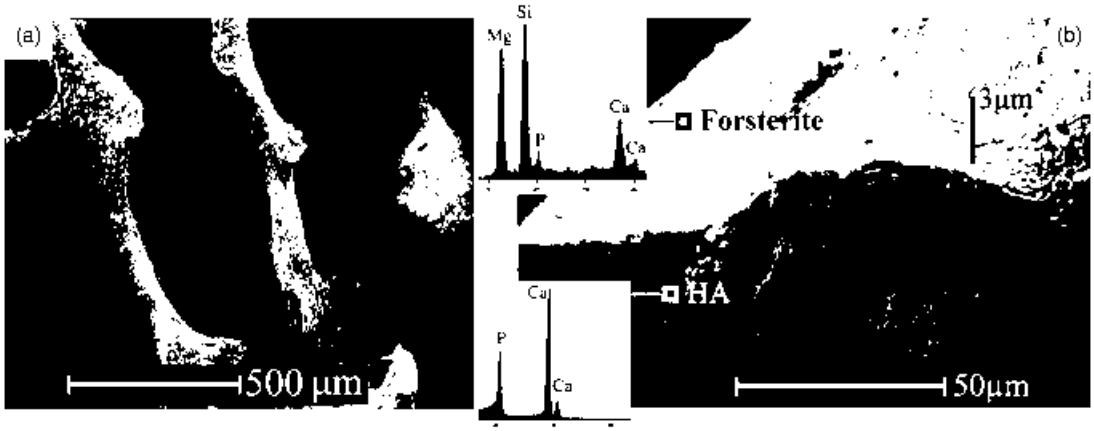

Fig. 5. Scanning electron microscopic micrographs and energy-dispersive spectrometer pattern of SC-1100: (a) Pore structure; (b) microstructure of strut.

A/W glass–ceramics with about 93% porosity. They could improve the compressive strength of the scaffold to ~1 MPa. Roohani *et al.*[23] developed PHA scaffolds coated with bioactive glass (58S) and enhanced the compressive strength from 0.2 to 1.49 MPa. It is obvious that the present nanostructured forsterite-coated HA foams (porosity: ~83%, compressive strength: 1.61 MPa) are in general stronger than the HA-based foams of similar porosities; moreover in this research, polymeric materials are not used as a coating material.

Also, *in vitro* bioactivity test shows that forsterite nanopowder is bioactive.[33] Our results indicate that the scaffolds obtained provided good mechanical support while maintaining bioactiv-

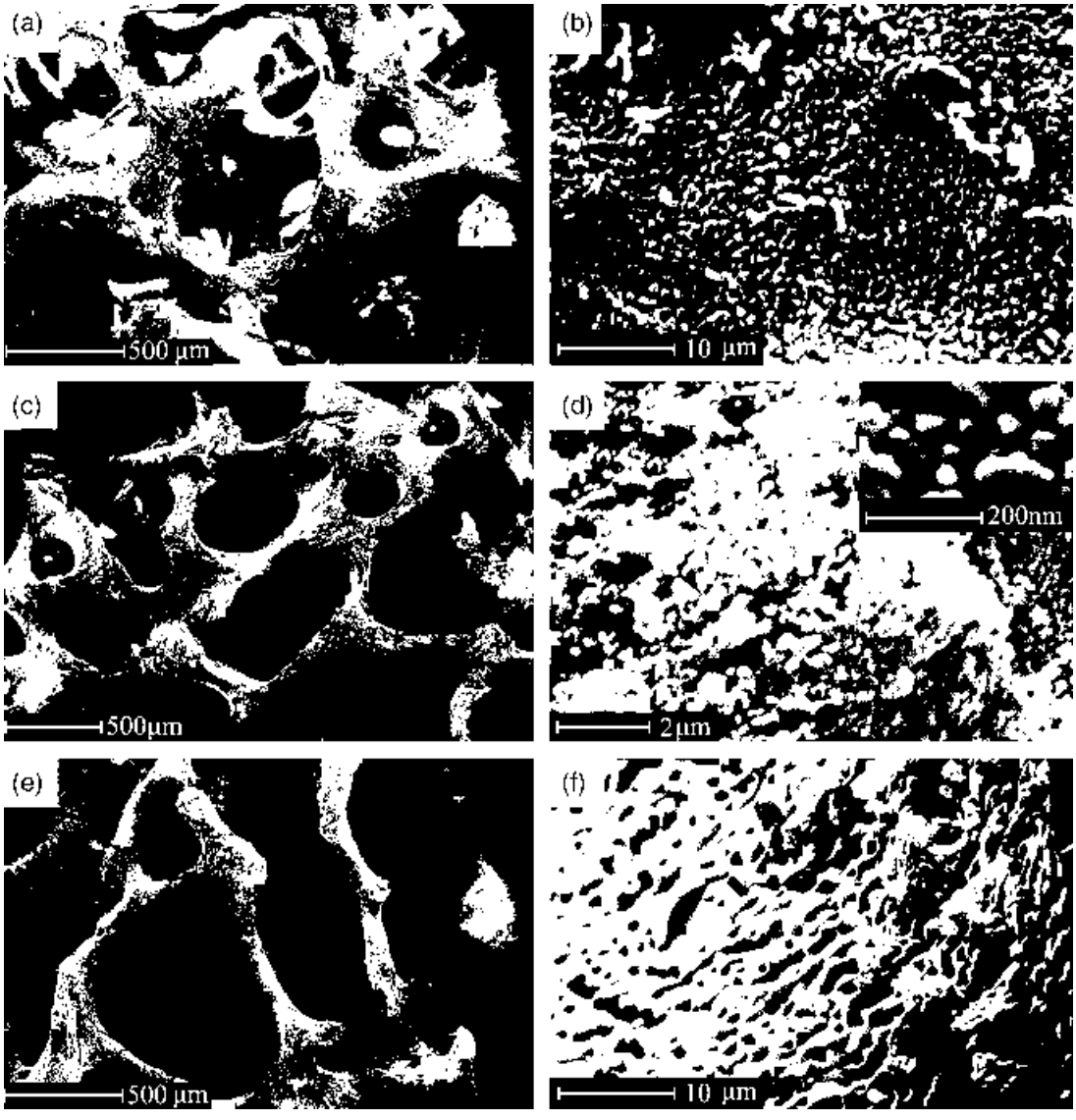

Fig. 6. Pore structure and microstructure of strut of (a, b) SC-HA; (c, d) SC-900; and (e, f) SC-1100.

ity, and hence they could be used as tissue engineering scaffolds for low-load-bearing applications.

IV. Conclusion

This work successfully synthesized novel, highly porous (porosity: ~83%, mean pore size: ~750 μm), mechanically competent, and nanostructured forsterite-coated HA scaffolds for bone engineering. It was found that initially the grain size of the coating increased from ~60 nm at 900°C to about 300 nm at 1000°C and thereafter increased to ~2 μm when sintered at 1100°C. A significant finding was that this simple method enhanced the compressive strength of porous HA from 0.12 to 1.61 MPa without using any polymeric materials.

References

[1]J. M. Karp, P. D. Dalton, and M. S. Shoichet, "Scaffolds for Tissue Engineering," *Mater. Res. Bull.*, **28**, 301–6 (2003).

[2]P. S. Eggli, W. Muller, and C. R. K. Schenk, "Porous Hydroxyapatite and Tricalcium Phosphate Cylinders with Two Different Pore Size Ranges Implanted in the Cancellous Bone of Rabbits," *Clin. Orthop. Relat. Res.*, **232**, 127–38 (1988).

[3]M. Doblaré, J. M. Garcia, and M. J. Gomez, "Modelling Bone Tissue Fracture and Healing: A Review," *Eng. Fract. Mech.*, **71**, 1809–40 (2004).

[4]R. Emadi, S. I. R. Esfahani, and F. Tavangarian, "A Novel, Low Temperature Method for the Preparation of β-TCP/HAP Biphasic Nanostructured Ceramic Scaffold from Natural Cancellous Bone," *Mater. Lett.*, **64**, 993–6 (2010).

[5]L. L. Hench and J. Wilson, *An Introduction to Bioceramics*. World Scientific, Singapore, 1993.

[6]J. J. Klawitter and S. F. Hulbert, "Application of Porous Ceramics for the Attachment of Load Bearing Orthopedic Applications," *J. Biomed. Mater. Res. Symp.*, **2**, 161–229 (1971).

[7]O. Gauthier, J. M. Bouler, E. Aguado, P. Pilet, and G. Daculsi, "Macroporous Biphasic Calcium Phosphate Ceramics; Influence of Macropore Diameter and Macroporosity Percentage on Bone Ingrowth," *Biomaterials*, **19**, 133–9 (1998).

[8]J. X. Lu, B. Flautre, K. Anselme, and P. Hardouin, "Role of Interconnections in Porous Bioceramics on Bone Recolonization In Vitro and In Vivo," *J. Mater. Sci. Mater. Med.*, **10**, 111–20 (1999).

[9]L. L. Hench, "Bioceramics," *J. Am. Ceram. Soc.*, **81**, 1705–33 (1998).

[10]W. Suchanek and M. Yoshimura, "Processing and Properties of Hydroxyapatite-Based Biomaterials for Use as Hard Tissue Replacement Implants," *J. Mater. Res.*, **13**, 94–117 (1998).

[11]R. W. Bucholz, A. Carlton, and R. Holmes, "Interporous Hydroxyapatite as a Bone Graft Substitute in Tibial Plateau Fractures," *Clin. Orthop. Relat. Res.*, **240**, 53–62 (1989).

[12]J. Zeltinger, J. K. Sherwood, D. A. Graham, R. Mueller, and L. G. Griffith, "Effect of Pore Size and Void Fraction on Cellular Adhesion, Proliferation, and Matrix Deposition," *Tissue Eng.*, **7**, 557–72 (2001).

[13]E. Damien, K. Hing, S. Saeed, and P. A. Revell, "A Preliminary Study on the Enhancement of the Osteointegration of a Novel Synthetic Hydroxyapatite Scaffold In Vivo," *J. Biomed. Mater. Res.*, **66**, 241–6 (2003).

[14]T. M. Freyman, I. V. Yannas, and L. J. Gibson, "Cellular Materials as Porous Scaffolds for Tissue Engineering," *Prog. Mater. Sci.*, **46**, 273–82 (2001).

[15]W. Y. Yeong, C. K. Chua, K. F. Leong, and M. Chandrasekaran, "Rapid Prototyping in Tissue Engineering: Challenges and Potential," *Trends Biotechnol.*, **22**, 643–52 (2004).

[16]K. A. Gross and L. M. Rodríguez-Lorenzo, "Biodegradable Composite Scaffolds with an Interconnected Spherical Network for Bone Tissue Engineering," *Biomaterials*, **25**, 4955–62 (2004).

[17]H. W. Kim, S. Y. Lee, C. J. Bae, Y. J. Noh, H. E. Kim, H. M. Kim, and J. S. Ko, "Porous ZrO_2 Bone Scaffold Coated with Hydroxyapatite with Fluorapatite Intermediate Layer," *Biomaterials*, **24**, 3277–84 (2003).

[18]Y. K. Jun, W. H. Kim, O. K. Kweon, and S. H. Hong, "The Fabrication and Biochemical Evaluation of Alumina Reinforced Calcium Phosphate Porous Implants," *Biomaterials*, **24**, 3731–9 (2003).

[19]V. S. Komlev, S. M. Barinov, and F. Rustichelli, "Strength Enhancement of Porous Hydroxyapatite Ceramics by Polymer Impregnation," *J. Mater. Sci. Lett.*, **22**, 1215–7 (2003).

[20]M. Peroglio, L. Gremillard, J. Chevalier, L. Chazeau, C. Gauthier, and T. J. Hamaide, "Toughening of Bio-Ceramics Scaffolds by Polymer Coating," *J. Eur. Ceram. Soc.*, **27**, 2679–85 (2007).

[21]X. Miao, L. P. Tan, L. S. Tan, and X. Huang, "Porous Calcium Phosphate Ceramics Modified with PLGA-Bioactive Glass," *Mater. Sci. Eng. C*, **27**, 274–9 (2007).

[22]X. Miao, G. Lim, K. H. Loh, and A. R. Boccaccini, "Preparation and Characterisation of Calcium Phosphate Bone Cement," *Mater. Proc. Prop. Perf.*, **3**, 319–24 (2004).

[23]S. I. Roohani Esfahani, F. Tavangarian, and R. Emadi, "Nanostructured Bioactive Glass Coating on Porous Hydroxyapatite Scaffold for Strength Enhancement," *Mater. Lett.*, **62**, 3428–30 (2008).

[24]I. K. Jun, J. H. Song, W. Y. Choi, Y. H. Koh, and H. E. Kim, "Porous Hydroxyapatite Scaffolds Coated with Bioactive Apatite–Wollastonite Glass–Ceramics," *J. Am. Ceram. Soc.*, **90** [9] 2703–8 (2007).

[25]T. Tian, D. Jiang, J. Zhang, and Q. Lin, "Fabrication of Bioactive Composite by Developing PLLA onto the Framework of Sintered HA Scaffold," *Mater. Sci. Eng. C*, **28**, 51–6 (2008).

[26]H. W. Kim and J. C. Knowles, "Hydroxyapatite Porous Scaffold Engineered with Biological Polymer Hybrid Coating for Antibiotic Vancomycin Release," *J. Mater. Sci. Mater. Med.*, **16**, 189–95 (2005).

[27]H. W. Kim, J. C. Knowles, and H. E. Kim, "Hydroxyapatite/poly(Epsilon-Caprolactone) Composite Coatings on Hydroxyapatite Porous Bone Scaffold for Drug Delivery," *Biomaterials*, **25**, 1279–87 (2004).

[28]C. Wu and J. Chang, "Synthesis and Apatite-Formation Ability of Akermanite," *Mater. Lett.*, **58**, 2415–7 (2004).

[29]H. S. Ryu, K. S. Hong, J. K. Lee, D. J. Kim, and J. H. Lee, "Magnesia-Doped HA/β-TCP Ceramics and Evaluation of their Biocompatibility," *Biomaterials*, **25**, 393–401 (2004).

[30]S. R. Kim, J. H. Lee, Y. T. Kim, D. H. Riu, S. J. Jung, Y. J. Lee, S. C. Chung, and Y. H. Kim, "Synthesis of Si, Mg Substituted Hydroxyapatites and their Sintering Behaviors," *Biomaterials*, **24**, 1389–98 (2003).

[31]T. J. Webster, E. A. Massa-Schlueter, J. L. Smith, and E. B. Slamovich, "Osteoblast Response to Hydroxyapatite Doped with Divalent and Trivalent Cations," *Biomaterials*, **25**, 2111–21 (2004).

[32]S. Ni, L. Chou, and J. Chang, "Preparation and Characterization of Forsterite (Mg_2SiO_4) Bioceramics," *Ceram. Int.*, **33**, 83–8 (2007).

[33]M. Kharaziha and M. H. Fathi, "Synthesis and Characterization of Bioactive Forsterite Nanopowder," *Ceram. Int.*, **35**, 2449–54 (2009).

[34]M. H. Fathi and M. Kharaziha, "Two-Step Sintering of Dense, Nanostructural Forsterite," *Mater. Lett.*, **63**, 1455–8 (2009).

[35]N. O. Engin and A. C. Tas, "Manufacture of Macroporous Calcium Hydroxyapatite Bioceramics," *J. Eur. Ceram. Soc.*, **19**, 2569–72 (1999).

[36]A. Bigi, G. Falini, E. Foresti, A. Ripamonti, M. Gazzano, and N. Roveri, "Magnesium Influence on Hydroxyapatite Crystallization," *J. Inorg. Biochem.*, **49**, 69–78 (1993).

[37]I. R. Gibson and W. Bonfield, "Preparation and Characterization of Magnesium/Carbonate Co-Substituted Hydroxyapatites," *J. Mater. Sci. Mater. Med.*, **13**, 685–93 (2002).

[38]S. Ramesh, C. Y. Tan, I. Sopyan, M. Hamdi, and W. D. Teng, "Consolidation of Nanocrystalline Hydroxyapatite Powder," *Sci. Technol. Adv. Mat.*, **8**, 124–30 (2007). □